Radiation Physics and Chemistry 91 (2013) 81–88

Contents lists available at SciVerse ScienceDirect

Radiation Physics and Chemistry

journal homepage: www.elsevier.com/locate/radphyschem

Investigation of Au^{9+} swift heavy ion irradiation on $CdS/CuInSe_2$ thin films

Rajesh A. Joshi [a,*], Vidya S. Taur [b], Fouran Singh [c], Ramphal Sharma [b,**]

[a] Department of Physics, Toshniwal Arts, Commerce and Science College, Sengaon, Dist. Hingoli 431542, Maharashtra, India
[b] Thin Film and Nanotechnology Laboratory, Department of Physics, Dr. Babasaheb Ambedkar Marathwada University, Aurangabad 431004, Maharashtra, India
[c] Material Science Division, Inter-University Accelerator Center (IUAC), New Delhi 110067, India

HIGHLIGHTS

- Nanostructured $CdS/CuInSe_2$ can be grown by chemical ion exchange method.
- Physicochemical and optoelectronic properties can be modified by 120 MeV Au^{9+} SHI Irradiation.
- Solar energy conversion efficiency improved from 0.26 to 1.59% in $CdS/CuInSe_2$ upon irradiation.

ARTICLE INFO

Article history:
Received 21 May 2012
Accepted 7 May 2013
Available online 14 May 2013

Keywords:
Ion exchange method
Nanostructured $CdS/CuInSe_2$ thin films
SHI irradiation
Physicochemical and optoelectronic properties

ABSTRACT

In the present manuscript we report about the preparation of $CdS/CuInSe_2$ heterojunction thin films by chemical ion exchange method and investigation of 120 MeV Au^{9+} swift heavy ions (SHI) irradiation effect on its physicochemical as well as optoelectronic properties. These pristine (as grown) samples are irradiated with 120 MeV Au^{9+} SHI of 5×10^{11} and 5×10^{12} ions/cm^2 fluencies and later on characterized for structural, compositional, morphological, optical and I–V characteristics. X-ray diffraction (XRD) pattern obtained from pristine and irradiated films shows considerable modifications in peak intensity as well as rising of some new peaks, corresponding to In_2Se_3, Cu_3Se_2 and $CuIn_2Se_3$ materials. Transmission electron microscope (TEM) images show decrease in grain size upon increase in irradiation ion fluencies, which is also supported from the observation of random and uneven distribution of nano-grains as confirmed through scanning electron microscope (SEM) images. Presence of Cd, Cu, In, S and Se in energy dispersive X-ray spectrum analysis (EDAX) confirms the expected and observed elemental composition in thin films, the absorbance peaks are related to band to band transitions and spin orbit splitting while energy band gap is observed to increase from 1.36 for pristine to 1.53 eV for SHI irradiated thin films and I–V characteristics under illumination to 100 mW/cm^2 light source shows enhancement in conversion efficiency from 0.26 to 1.59% upon irradiation.

1. Introduction

The compounds of I–III–IV_2 group elements have attracted much attention in recent years due to their potential electronic and optical properties which make them suitable for various device grade applications (Chopra et al., 2004, Kessler et al., 2003, Mobarak et al., 2008). Among them, $CdS/CuInSe_2$ is considered as a promising material for solar cell, owing to its synthesis dependant, composition controlled tunable optoelectronic properties. Although there are numerous physical and chemical methods available for the synthesis of nanostructured $CdS/CuInSe_2$ thin films, but achieving desired stiochiometry, stability and energy conversion efficiency are the topics of great concern, requiring extensive research. Nevertheless, issues related to stiochiometry and stability of thin films can be resolved up to certain extent by using chemical ion exchange technique (Sharma et al., 2009a, 2009b), but improvising of lower values of conversion efficiency remains a challenge, extending scope of the work (Kehan et al., 2009, Scheer et al., 2010, Yoon et al., 2009). As solar energy conversion is surface, interface and composition dependent phenomenon, hence surface, interface and composition can be modified by providing post deposition treatments like annealing under different ambient conditions or swift heavy ion (SHI) irradiation (Chandramohan et al., 2009, Gokulakrishnan et al., 2012, Hedler

* Corresponding author. Tel.: +91 9096655278.
** Corresponding author. Tel.: +91 9422793173, +91 240 2401365; fax: +91 240 2403115/2403335.
E-mail addresses: urajoshi@gmail.com, uraj_joshi@yahoo.com (R.A. Joshi), ramphalsharma@yahoo.com (R. Sharma).

0969-806X/$ - see front matter © 2013 Elsevier Ltd. All rights reserved.
http://dx.doi.org/10.1016/j.radphyschem.2013.05.005

et al., 2005, Mallick et al., 2008, Prakash et al., 2011, Sharma et al., 2009a, 2009b, Trautmann, 1999). To the best of our knowledge there are some literatures available about effect of radiation on $CuInSe_2$ and other binary compounds showing significant modifications in the properties of the material (Ashry et al., 2001, Sathyamoorthy et al., 2006, Tanaka et al., 2003), but rarely there may be any literature available mentioning about the use of SHI irradiation for surface, interface and composition modifications in nanostructured $CdS/CuInSe_2$ heterojunction thin films intended for solar cell applications. Thus with this motivation, in the present work we have used the chemical ion exchange method for synthesis of stiochiometric, homogenous interface and stable nanostructured $CdS/CuInSe_2$ thin films.

Therefore in the present work, we report about the investigation of Au^{9+} SHI irradiation on the structural, compositional, optical, electronic and I–V characteristics of $CdS/CuInSe_2$ thin films. These films are prepared using chemical ion exchange method at room temperature in two stages and later on irradiated using 120 MeV Au^{9+} SHI of two fluencies 5×10^{11} and 5×10^{12} ions/cm^2. These pristine and irradiated thin films were further characterized using X-ray diffractometer (XRD), transmission electron microscopy (TEM), energy dispersive X-ray analysis (EDAX), scanning electron microscopy (SEM), UV–Vis absorbance spectra and I–V characteristics.

2. Experimental details

The heterojunction $CdS/CuInSe_2$ thin films are grown in two stages, in first stage CdS is grown on ITO substrate by chemical bath deposition method and in the next stage $CuInSe_2$ is deposited over ITO/CdS by chemical ion exchange method. Here, CdS is prepared using 0.02 M cadmium chloride ($CdCl_2$) and 0.03 M thiourea ($CS(NH_2)_2$), as sources of Cd^{2+} and S^{2-} respectively. These reactants are mixed in equal quantity in a beaker at a reaction temperature of 80 °C under controlled pH ~11 monitored by the addition of ammonia in reaction bath. Two to three drops of tri-ethanolamine ($C_6H_{15}NO_3$) is added to the cadmium source so as to reduce the formation of metal oxide (Joshi et al., 2011). The reaction is carried for 1 h to form orange color (physical appearance) at the ITO substrate surface. These CdS deposited ITO substrates are used for $CuInSe_2$ deposition by ion exchange method using 0.02 M copper sulfate ($CuSO_4$), 0.02 M indium trichloride ($InCl_3$) and 0.04 M sodium seleno-sulfate (Na_2SeSO_3) (Sharma et al., 2009a, 2009b). The indium tri-chloride ($InCl_3$) is prepared in citric acid, while sodium seleno-sulfate (Na_2SeSO_3) is prepared by refluxing the elemental selenium (Se) in sodium sulfate (Na_2SO_4) at 80 °C for 5 h. The chemical ion exchange reaction is carried at room temperature by mixing the Cu, In and Se source solutions in a beaker in equal volumetric proportion, in which CdS deposited ITO substrates are also immersed to obtain $ITO/CdS/CuInSe_2$ configuration. The resultant heterojunction may form homogenous interface between CdS and $CuInSe_2$ due to surface ionic exchange of cations and anions (Sharma et al., 2009a, 2009b). However, to further improve the physicochemical and optoelectronic properties of these heterojunction thin films, SHI irradiation using 120 MeV Au^{9+} ions of 5×10^{11} and 5×10^{12} ions/cm^2 were performed.

The literature survey has shown that; above certain threshold values of electronic stopping power; the high energy heavy ions are capable of changing the physical and compositional properties of the materials (Krasheninnikov et al., 2010, Kucheyev et al., 2011). Considering these facts and energy loss by 120 MeV Au ions; it is observed that the energy loss is dominated by electronic energy loss in $CdS/CuInSe_2$ system as simulated using SRIM 2003 code. Two 1 × 1 cm^2 size targets of $ITO/CdS/CuInSe_2$ thin films were mounted on the copper ladder for SHI irradiation experiments and the ladder was placed vertically in the chamber maintained at high vacuum (HV) of 2.1×10^{-6} Torr, the angle of SHI incidence was normal to the surface of the target thin films. Temperature of the system was maintained at 300 K during irradiation, 120 MeV Au^{9+} ions available from 15 UD Pelletron accelerators at IUAC, New Delhi, India, were scanned over the targets using electrostatic scanner. The target thin films were exposed to ion beam for fluences of 5×10^{11} and 5×10^{12} ions/cm^2. A negative 120 V was applied on the suppressor around copper ladder to suppress secondary electrons generated during the irradiation process.

Hence such pristine and irradiated thin films of $CdS/CuInSe_2$ are characterized for structural, compositional, morphological, optical and electrical properties. The structural analysis is performed using X-ray diffraction (XRD) patterns obtained from the films recorded on Bruker AXS, German (D-8 Advanced) diffractometer in the scanning range 20–60° (2θ) using Cu $K\alpha_1$ radiations with wavelength of 1.5405 Å. Raman spectra were obtained using laser beam at wavelength of 514.5 nm (5 mW) from an argon ion laser and data recorded between 100 and 1400 cm^{-1} at room temperature on Renishaw In-via Raman microscope. Transmission electron microscopy (TEM) images were obtained using JEM 2000 EXII. The compositional and surface morphology analysis was carried out by energy dispersive X-ray (EDAX) facility attached scanning electron microscopy (SEM) instrument, JOEL-JSM-5600. To study the optical properties of the films, absorbance spectra were recorded in 400–1100 nm range using UV–Vis spectrophotometer Perkin Elmer Lamda-25. The solar energy conversion efficiency experiments were performed by illuminating these thin films to 100 mW/cm^2 light source by acquiring the data on Lab-Equip I–V measurement setup 2004 interfaced with computer. Correlations between SHI irradiation and the photo conversion capability were studied and results are reported in the present paper.

3. SHI irradiation effect

Use of SHI for material modifications is an efficient post deposition treatment, which enables controlled compositional and surface modification in the materials (Shirai et al., 2009). In this process, an ion impinged on the surface of the thin film, loses its energy in the form of inelastic collisions, which may be used for excitation of electrons from films (materials) atomic levels (Srivastava et al., 2003). These inelastic collisions result in ionization of the charge carriers and atoms from their molecular levels, which makes drastic change in the material by displacing ions from the surface and mixing at an interface. These ionic displacements create vacancies and defects in the material along with the creation of ion tracks which may correspond to the surface modifications (Awasthi, 1997). Although in the present study we are unable to identify diameter of the ion tracks but literature had revealed track diameter between 40 and 100 nm (Krasheninnikov et al., 2010, Moll et al., 2010). Formation of such heavy energy ion tracks indicate melting, sputtering and resolidifications of material to form new bonds, leading towards material modification (Bringa et al., 2002). Here in the present case, irradiation of the $CdS/CuInSe_2$ surface by SHI causes material modifications in the form of creation of new structural compositions like Cu_3Se_2, In_2Se_3 and $CuIn_2Se_3$, which are confirmed using XRD. During the electronic energy loss, ions interact with $CuInSe_2$ material, which dissociates to form new bonds, such as

$$4CuInSe_2 \xrightarrow{SHI} Cu_3Se_2 + In_2Se_3 + CuIn_2Se_3 \quad (1)$$

These newly generated materials confirm the compositional modifications upon SHI treatments.

4. Results and discussion

4.1. XRD analysis

The X-ray diffraction (XRD) patterns obtained from pristine and irradiated CdS/$CuInSe_2$ thin films are shown in Fig. 1. Peaks observed at (1 1 2), (2 0 4) and (2 2 0) in the diffraction pattern confirm the formation of $CuInSe_2$ phase which is in good agreement with standard JCPDS data card 81-1936, while peak at 21.40° suggests the presence of CdS, which is found to be stable even after irradiation treatment (Chandramohan et al., 2009). XRD pattern of the irradiated CdS/$CuInSe_2$ thin films shows significant change in peak intensity along with appearance of some new peaks which could be assigned for In_2Se_3, Cu_3Se_2 and $CuIn_2Se_3$ (JCPDS data cards 71-0250, 19-0402 and 35-1349). The rising of these three new peaks may be due to mixing of indium (In) and selenium (Se), which might have been liberated from the tightly bonded chalcopyrite structure as they require high energy for formation provided through the irradiation process (Kuznetsov et al., 2003; Sathyamoorthy et al., 2006). Such new bonds in the CdS/$CuInSe_2$ thin films lead to structural modification which could be counted by δ (ratio of c/2a) (Shay et al., 1973). For irradiated thin films, the δ value is found to be shifted towards unity (i.e. 1.04, 1.01 and 1.00 for pristine and irradiated for 5×10^{11}, 5×10^{12} ions/cm^2 respectively), which confirms material modification on irradiation treatment (Tanino et al., 1992). Even the effect is also observed on structural geometry i.e. tetrahedral distortion, which is represented by Δx, when the anion is distorted from its ideal tetrahedral position due to strain induced by the formation of In_2Se_3, Cu_3Se_2 and $CuIn_2Se_3$ bonds. The strain is observed to increase as the irradiation dose is increased from 0.007, 0.022 to 0.035 for pristine and irradiated for 5×10^{11}, 5×10^{12} ions/cm^2 respectively, which is calculated from the following equation:

$$\varepsilon = \frac{d_{observed} - d_{standard}}{d_{standard}} \quad (2)$$

where $d_{standard}$ is the standard value of inter planer spacing and $d_{observed}$ is the inter planer lattice spacing observed experimentally, the strain increases from 10^{-3} to 10^{-2} even when strain results in misbalancing of bond length L_{AC} and L_{BC} i.e. the distance between the first nearest neighbor of anion C and other two elements A and B (Cu and In) (Tanino et al., 1992). The peak ratio of (1 1 2) to (2 2 0) is observed to be increased from 2 to 4.82 corresponding for crystallographic modifications (Mallick et al., 2008) and the other calculated structural parameters are also tabulated in Table 1.

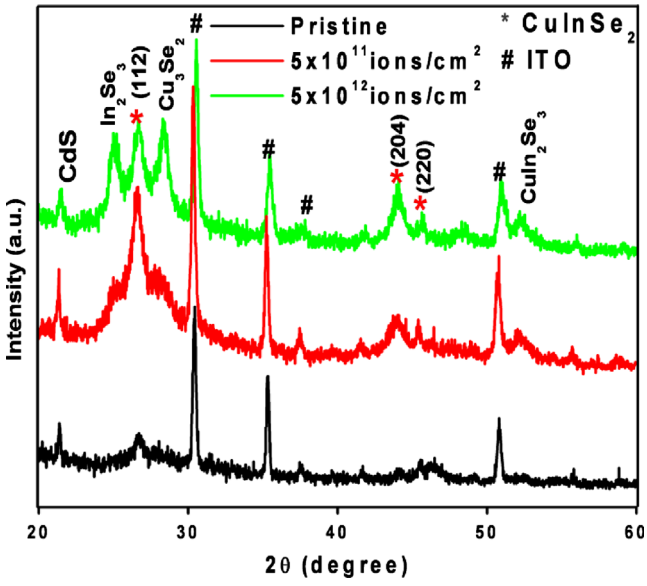

Fig. 1. XRD patterns of pristine and 120 MeV Au^{9+} SHI irradiated nanostructured CdS/$CuInSe_2$ heterojunction thin films.

4.2. Raman spectrum analysis

Fig. 2 represents the Raman spectra obtained from pristine and irradiated CdS/$CuInSe_2$ thin films which can be co-related with the structural modifications observed from XRD pattern. The Raman optic active modes of chalcopyrite structure can be expressed as $1A_1+3B_1+3B_2+6E$ where A_1 corresponds for the movement of anion (Se) in $CuInSe_2$ domain, while B and E are related to the optical vibrational modes (TO and LO) of CdS/$CuInSe_2$ lattice (Ming et al., 2006). Peaks obtained at 170 cm^{-1} could be assigned to A_1 vibrational mode. On SHI irradiation, shift in Raman peak position is observed in addition to a shoulder peak at 281 cm^{-1} characterizing the presence of CuSe phase (Zaretskaya et al., 2003). Peak obtained at 1022 cm^{-1} corresponds for ITO glass which is used as substrate. The symmetry of observed modes was assigned for the polarization and composition dependence of the material. As in Fig. 2, large shift and broadening of peaks in Raman spectra of irradiated films are observed, which indicates that excitation of vibrational mode might be induced by substitutional disorder. Significant broadening and decrease in the intensity of A_1 mode is an indicative of material modifications resulting in the improvement of crystalline quality (Gan et al., 1976). Shift of A_1 mode confirms variation of Cu percentage in the thin film and creation of charge neutral defect pair ($2V_{Cu}^{-}+In_{Cu}^{2+}$) which may lead to modifications from non-polar (2 2 0) to polar (1 1 2) surface (Ming et al., 2006). So it may be inferred that, the film has combination of Cu deficient and Cu rich nano-domains. Such different Cu, In and Se concentrations can create different local environment in crystal structure. When Cu and In are partially substituted from the $CuInSe_2$ compound on SHI irradiation to raise Cu_3Se_2, In_2Se_3 and $CuIn_2Se_3$, the compositional variations become responsible for non-linear shift of A_1 mode (Ming et al., 2006). Here, shift and broadening of A_1 mode with appearance of new peaks confirm structural and compositional modifications (Gan et al., 1976; Mallick et al., 2008). This compositional modification induces stress in chalcopyrite lattice (Zaretskaya et al., 2007),

Table 1
Structural parameters estimated from the XRD pattern of pristine and SHI irradiated CdS/$CuInSe_2$ heterojunction thin films with 120 MeV Au^{9+} ions of 5×10^{11} ions/cm^2 and 5×10^{12} ions/cm^2 fluencies.

Type	a	c	c/a	δ	Δx	L_{AC} (Å)	L_{BC} (Å)	d (std)	d (obs)	e	$I_{(112)}/I_{(220)}$	D (nm)
Pristine	5.58	11.67	2.09	1.04	0.22	2.38	2.52	3.3453	3.3695	7.1×10^{-3}	2	27
Irradiated 5×10^{11} ions/cm^2	5.72	11.66	2.03	1.01	0.24	2.46	2.48	3.3453	3.4205	2.2×10^{-2}	3.22	19
Irradiated 5×10^{12} ions/cm^2	5.74	11.56	2.01	1.00	0.24	2.48	2.50	3.3453	3.4630	3.4×10^{-2}	4.82	17

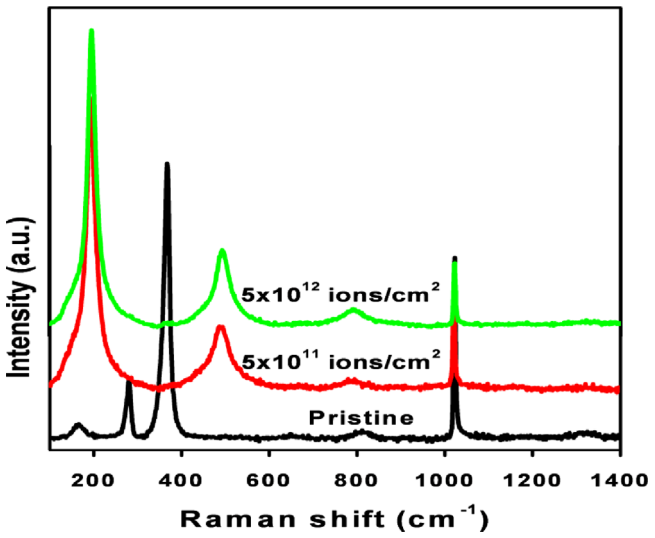

Fig. 2. Raman spectra obtained from pristine and 120 MeV Au^{9+} SHI irradiated nanostructured CdS/$CuInSe_2$ thin films.

Table 2
Characteristic Raman peak position and other parameters calculated from Raman vibrational spectra obtained from pristine and SHI irradiated CdS/$CuInSe_2$ heterojunction thin films with 120 MeV Au^{9+} ions of 5×10^{11} ions/cm^2 and 5×10^{12} ions/cm^2 fluencies.

Type	Raman peak (cm^{-1})	FWHM (cm^{-1})	Area ratio	Stress (MPa)
Pristine	163	23.16	1	0
Irradiated 5×10^{11} ions/cm^2	194	18.68	0.028	729
Irradiated 5×10^{12} ions/cm^2	196	17.23	0.018	753

which can be calculated using (Srikar et al., 2003, Wolf, 1996);

$$\sigma(MPa) = -250(\omega_s - \omega_o) \quad (3)$$

where ω_s and ω_o are the positions of Raman shift for pristine and irradiated thin films respectively. Decrease in full width at half maxima (FWHM) of Raman peak and ratio of area under the peaks for irradiated and pristine samples confirm improvement in crystallinity of the material. The stress is observed to increase till 753 MPa (Budak et al., 2012; Mallick et al., 2008; Parthiban et al., 2011). The other parameters calculated from Raman spectra are tabulated in Table 2.

4.3. TEM study

Fig. 3(a)–(c) represents transmission electron microscopy (TEM) images while inset shows selected area electron diffraction (SAED) pattern of pristine and irradiated thin films. From TEM images, distinct dark spots are observed to be uniformly distributed throughout the sample indicating its homogeneity and SAED shows diffused ring pattern which is characteristic of polycrystalline material (Joshi et al., 2011). This provides the confirmation that films are composed of nanocrystalline $CuInSe_2$ phase oriented to specific (1 1 2) direction. The SAED pattern of irradiated thin films shows disturbance in ring symmetry comparing with the inset of Fig. 3(a), images of Fig. 3(b) and (c) shows diverse diffractions which may be related to composition modification upon irradiation. Even the spots of varying brightness are also observed as in TEM and SAED profiles indicating that there are

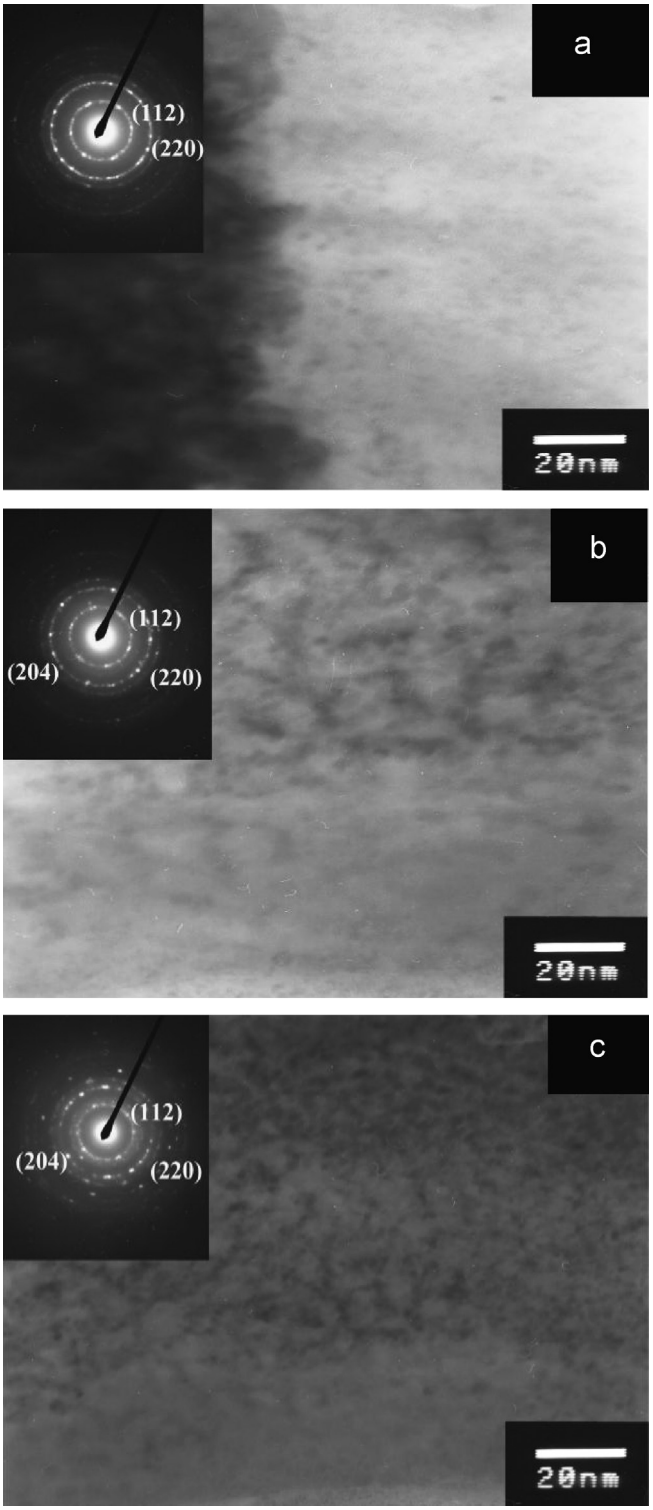

Fig. 3. TEM images and inset shows SAED pattern of (a) pristine and SHI irradiated with (b) 5×10^{11} and (b) 5×10^{12} ions/cm^2 nanostructured CdS/$CuInSe_2$ thin films.

crystallites with different grain sizes around which most of the crystallites of the nanocrystalline phase might be distributed in the film. This may presumably be due to the different sizes of nanocrystalline particles observed at the film surface, and within the volume below the surface. However, it may also be due to different composition and stiochiometry of the film (Matsumura et al., 2005).

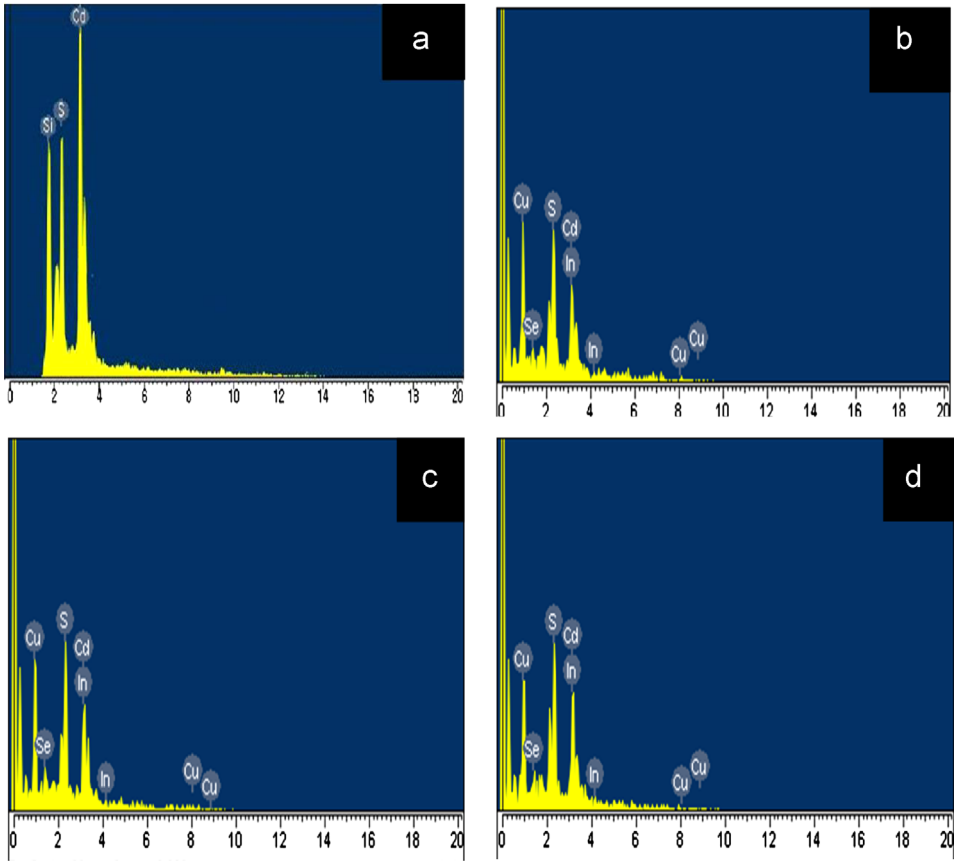

Fig. 4. EDAX spectra of (a) CdS, (b) pristine and 120 MeV Au^{9+} SHI irradiated with (b) 5×10^{11} and (b) 5×10^{12} ions/cm^2 nanostructured CdS/$CuInSe_2$ thin films.

4.4. Compositional analysis

The compositional study was carried, to obtain the elemental composition in CdS, and CdS/$CuInSe_2$ pristine and irradiated thin films using energy dispersive X-ray spectrum (EDAX) as shown in Fig. 4(a)–(d). From Fig. 4(a), the presence of cadmium (Cd) and sulphur (S) confirms the expected and obtained elements in thin films while the elemental proportion of Cd:S is obtained to be 55:45 confirming stiochiometry of CdS thin film. Fig. 4(b)–(d) represents the EDAX spectra obtained from pristine and irradiated CdS/$CuInSe_2$ thin films, the occurrence of significant peak for elements like Cd, Cu, In, S and Se confirms the contribution of expected composition in thin films, on the other hand a minute variation in the elemental proportions is observed in irradiated thin films which can be related to the breaking of $CuInSe_2$ molecule and formation of new bonds, which can create fluctuations in the elemental composition. Variation in Cd, Cu, In, S and Se elements affirm that the irradiation induces high energy deposition in the materials due to which the elemental displacement could occurs (Mallick et al., 2008). These obtained values are tabulated in Table 3.

4.5. Morphological analysis

Fig. 5(a)–(c) shows SEM images of pristine and SHI irradiated CdS/$CuInSe_2$ thin films. The images show variation in the crystallographic morphology and surface of the samples on SHI irradiation treatment (Gokulakrishnan et al., 2012; Mallick et al., 2012). When the observations are correlated with XRD patterns, the calculated intensity ratio of I(1 1 2): I(2 2 0) is found to increase from 2 to 4.82, which indicates the increase in crystallization and may be attributed to high temperature induced by SHI irradiation along the path of ions. From these observations, it is evident that higher fluence of SHI irradiation improves the crystallinity and quality of the films (Mallick et al., 2008, Shirai et al., 2009).

Table 3
The elemental composition analyzed from the EDAX spectra obtained from pristine and 120 MeV Au^{9+} SHI irradiated using 5×10^{11} ions/cm^2 and 5×10^{12} ions/cm^2 fluencies of CdS/$CuInSe_2$ thin films.

Elements	Cu K	Cd L	In L	S K	Se L
Sample					
Pristine	18.50	13.55	15.89	23.42	28.64
Irradiated 5×10^{11} ions/cm^2	17.84	13.13	15.91	22.87	30.25
Irradiated 5×10^{12} ions/cm^2	18.08	12.15	16.28	21.95	31.54

4.6. Optical analysis

The thin film of $CuInSe_2$ is used as an absorber layer for p–n junction solar cells, thus understanding that the optical properties related to electronic transitions and surface region has been considered to be crucial, where the junction formation takes place at an interface between $CuInSe_2$/CdS layers. Spectroscopic absorbance measurement of these thin films reveal that there are significant differences in optical properties and electronic transitions in pristine and irradiated thin films (Kilarkaje et al., 2011). The difference can be explained on the basis of reduction in Cu contents as a result of application of high energy provided through SHI irradiation process (Han et al., 2006). From the optical absorbance spectra as shown in Fig. 6, we observed reduction in absorbance strength of irradiated CdS/$CuInSe_2$ thin films as compared to the pristine one. The absorbance peaks obtained in the spectra can be related to band to band transitions and spin orbit

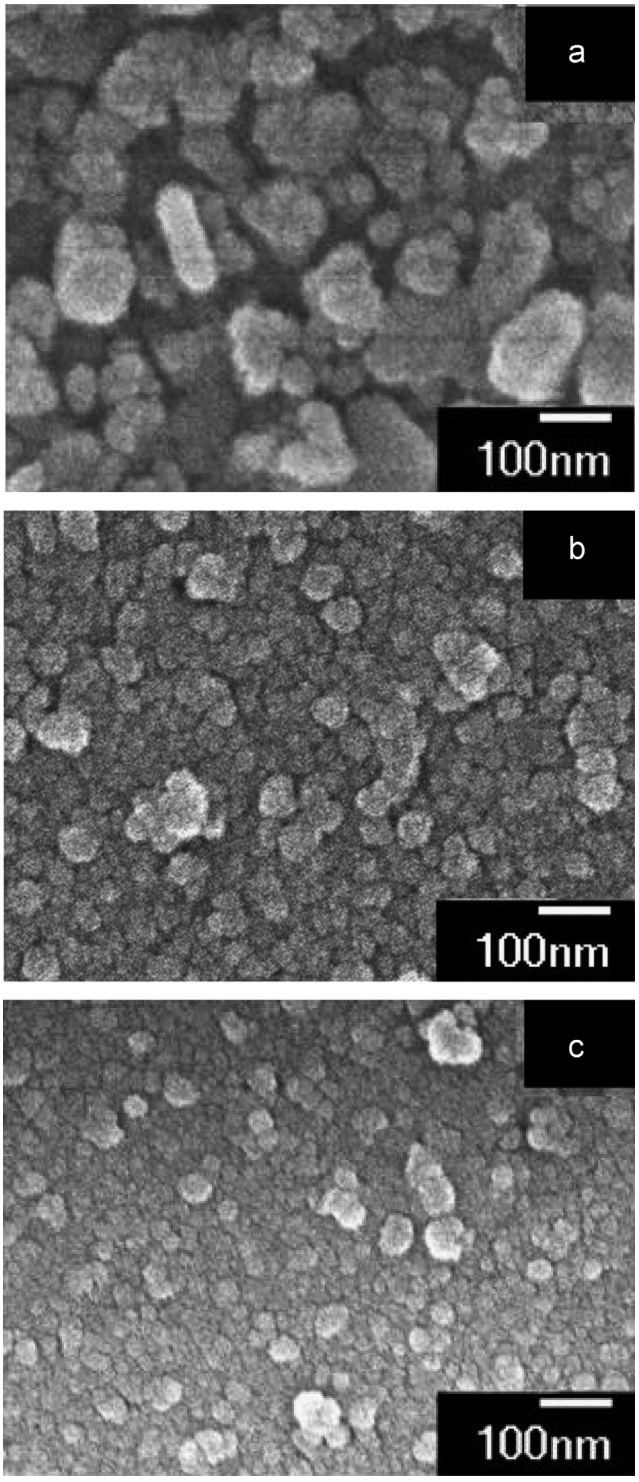

Fig. 5. SEM images obtained from CdS/$CuInSe_2$ thin films (a) Pristine and irradiated with (b) 5×10^{11} ions/cm^2 and (c) 5×10^{12} ions/cm^2.

splitting. Variation in spin orbit interaction between Cu and Se of $CuInSe_2$ is expected to be the main cause for observed shift in the absorbance band edge. The *p–d* hybridization in $CuInSe_2$ is supposed to be the cause for reducing spin–orbit interaction in the chalcopyrite $CuInSe_2$ thin film, which can also be explained in terms of density of Cu 3*d* and Se 4*p* states. Nevertheless, the effect of this hybridization is clearly reflected in the energy band gap value of the $CuInSe_2$ thin film. Inset in Fig. 6 shows plot of $(\alpha h\upsilon)^2$ versus $h\upsilon$ for calculation of energy band gap (Eg), which confirms

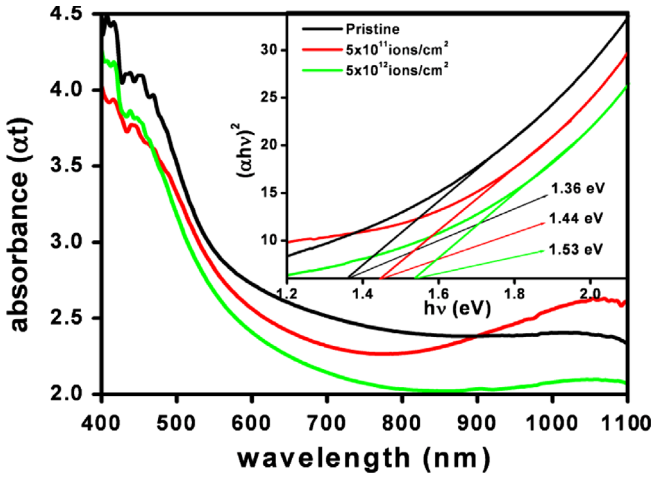

Fig. 6. The optical absorbance spectra obtained from pristine and 120 MeV Au^{9+} SHI irradiated CdS/$CuInSe_2$ thin films while inset shows energy band gap plot between $(\alpha h\upsilon)^2$ versus $h\upsilon$ (eV) calculated from the absorbance spectra.

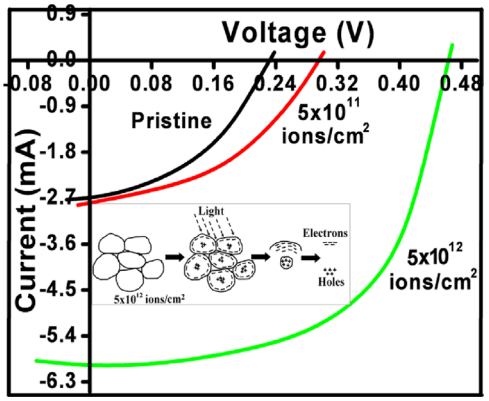

Fig. 7. I–V curve obtained from pristine and 120 MeV Au^{9+} SHI irradiated nanostructured CdS/$CuInSe_2$ thin films under illumination to 100 mW/cm^2 light source and inset Fig. shows schematic of electron hole pair separations as a consequence of grain boundary phenomenon.

Table 4
The optoelectronic parameters obtained from pristine and SHI irradiated CdS/$CuInSe_2$ heterojunction thin films with 120 MeV Au^{9+} ions of 5×10^{11} ions/cm^2 and 5×10^{12} ions/cm^2 fluencies.

Type	Eg (eV)	Δ_{CF}	Voc (V)	Isc (mA)	FF (%)	η (%)
Pristine	1.36	−0.09	0.2317	2.6574	41.50	0.26
Irradiated 5×10^{11} ions/cm^2	1.44	−0.03	0.2964	2.8021	41.65	0.36
Irradiated 5×10^{12} ions/cm^2	1.53	−0.01	0.4634	5.93	57.39	1.59

the increase in energy band gap values from 1.36 to 1.53 eV, and can be attributed to reduced *p–d* interaction in Cu and Se ions in irradiated $CuInSe_2$ domains (Han et al., 2006). According to the band theory and results available in the literatures about electronic transitions in I–III–VI_2 group compound ($CuInSe_2$), the upper valence band is formed exclusively by *p–d* hybridization of Cu 3*d* and Se 4*p*, whereas the In cations are not involved in band formation (Ghosh et al., 1990, Han et al., 2006, Shay et al., 1973). The strength of *d–p* interaction depends inversely on the energy of separation between Cu 3*d* orbital and Se 4*p* orbital. This repulsive interaction pushes the anti-bonding *p–d* states that constitute the valence band maxima (VBM) to higher energies. The VBM is composed of Cu 3*d* orbital that is hybridized with Se 4*p* orbital. However, in case of Cu-deficient irradiated $CuInSe_2$ thin film,

p–d repulsion is expected to be less than that of stiochiometric $CuInSe_2$ thin film. The effect of decrease in this repulsive interaction would be lowering of VBM as well as reducing the conduction band minima (CBM). Such reduction in VBM can be calculated in terms of crystal field splitting using the formula (Shay et al., 1973)

$$\Delta_{CF} = 2 - \left(\frac{c}{a}\right) \quad (4)$$

The observed values are found to be lower and negative i.e. −0.9 to −0.1, which can be due to the large compressive distortion produced in the $CuInSe_2$ lattice on SHI irradiation, hence, we can expect increase in band gap energy for irradiated $CuInSe_2$ thin films, the Eg increases from 1.36 to 1.53 eV. This observed increase in band gap energy after SHI irradiation treatment may be significant in achieving an enhancement in light conversion efficiency of heterojunction solar cells.

4.7. Solar cell characteristics

Fig. 7 shows plot of I–V characteristics of pristine and SHI irradiated nanostructured CdS/$CuInSe_2$ heterojunction thin films under illumination of 100 mW/cm^2 light source and the conversion efficiency is calculated using following formula (Sato et al., 2005):

$$\eta(\%) = \frac{P_{\max}}{P_{in}} \times 100 \quad (5)$$

where P_{max} is the maximum output power obtained and P_{in} is the input power applied and the conversion efficiency is found to increase from 0.26 to 1.59% as the irradiation fluence is increased (Budak et al., 2012). The solar cell efficiency and other optoelectronic parameters obtained are tabulated in Table 4. The observed increase in the conversion efficiency can be co-related with improved crystallinity, surface and interface of the CdS/$CuInSe_2$ thin-films on SHI treatments (Yan et al., 2006). In the pristine CdS/$CuInSe_2$ thin film, the surface morphology observed through the SEM image as in Fig. 5(a) shows non-uniform, un-even and hazy grains located away from each others on the surface, while, on SHI treatment the surface modification is observed, revealing an increase in compactness of the surface along with the grains interconnections as in Fig. 5(b) and (c). The observed grains are expected to be the cause for enhancement in conversion efficiency by the phenomenon of grain boundary charge transportations. These grain modifications form an effective charge separation centers for the optically generated electrons and holes. On exposure to light; surface region of thin films becomes negatively charged, while interior of the grains becomes positively charged which indicates increase in electron and hole density in the core and outer part of the grains (Persson et al., 2003) as shown in pictorial presentation in the inset of Fig. 7. Post deposition treatment to $CuInSe_2$ thin films also offer a scenario where anion vacancy V^{+}_{Se} (donor) drives out Cu and forms a dipolar complex neutral defect pair ($2V^{-}_{Cu}+In^{2+}_{Cu}$). The generation of such Cu rich and Cu deficient nano-domain with charged surface on irradiated $CuInSe_2$ thin films is system dependant. Furthermore, the existence of electron hole separator in $CuInSe_2$ and the creation of cation poor surface results in an increase in the density of negatively charged acceptors at the surface. Such charged surface defects in CdS/$CuInSe_2$ might be responsible for surface reconstruction and lowering of the valence band at the surface of these grains, which restrict holes from entering inside it. So the re-arrangement at grain surface might repel holes, thus, creating charge free zone at the grain surface leading to fast electron transport at the surface (Yan et al., 2006). Presence of such high density of holes in the interior with negatively charged surfaces of these grains might be considered to be affecting the valence-band offset. So creation of such potential barrier at the surface for holes can impede electron–hole recombination, which results in dissociation (separation) of photo generated electron–hole pairs. These separations of electron hole pair in high dose 5×10^{12} ions/cm^2 CdS/$CuInSe_2$ thin films give rise to the enhancement in the energy conversion efficiency of the device.

5. Conclusions

In the present paper, heterojunction CdS/$CuInSe_2$ thin films are prepared by chemical ion exchange method and effect of 120 MeV Au^{9+} SHI irradiation on physicochemical and optoelectronic properties specifically in line to solar cell are studied. The irradiated films exhibited increase in conversion efficiency from 0.26 to 1.59% upon exposure to 100 mW/cm^2 light source. The enhancement in conversion efficiency may be attributed to SHI induced surface, interface, structural and compositional modifications, as supported by XRD, Raman, TEM and SEM analysis. Blue shift in the optical energy band gap observed from 1.36 to 1.53 eV corresponds to the irradiation induced band distributions. The observed results confirm that SHI irradiation can be used for modification of physicochemical as well as optoelectronic properties of CdS/$CuInSe_2$ heterojunction thin film based solar cells.

Acknowledgments

The authors are thankful to IUAC, New Delhi (India) for SHI irradiation, characterization and the financial support through project IUAC/XIII.7/UFR-47304/2714 and Dr. Anil V. Ghule, Asst. Professor, Department of Nanotechnology, Dr. Babasaheb Ambedkar Marathwada University, Aurangabad for helpful discussion and characterizations.

References

Ashry, M., et al., 2001. Radiation effects on fabricated Cu_2S/CdS heterojunction photovoltaic cells. Renew. Energy 23, 441.
Awasthi, D.K., 1997. Role of swift heavy ions in materials characterization and modification. Vaccum 48, 1011.
Bringa, E.M., et al., 2002. Coulomb explosion and thermal spikes. Phys. Rev. Lett. 88, 165501.
Budak, S., et al., 2012. MeV Si ions bombardments effects on thermoelectric properties of SiO_2/SiO_2+Ge nanolayers. Radiat. Phys. Chem. 81, 410.
Chandramohan, S., et al., 2009. High energy heavy ion induced physical and surface chemical modifications in polycrystalline cadmium sulphide thin films. Appl. Phys. A 94, 703.
Chopra, K.L., et al., 2004. Thin-film solar cells: an overview. Prog. Photovoltaics Res. Appl. 12, 69.
Gan, J.N., et al., 1976. Raman and infrared spectra of the $(CuInSe_2)_{1-X}(2ZnSe)_X$ system. Phys. Rev. B 13, 3610.
Ghosh, D.K., et al., 1990. Characterization of some quaternary defect chalcopyrites as useful nonlinear optical and solar-cell materials. Phys. Rev. B 41, 5126.
Gokulakrishnan, V., et al., 2012. Investigation of O^{7+} swift heavy ion irradiation on molybdenum doped indium oxide thin films. Radiat. Phys. Chem. 81, 589.
Han, S.H., et al., 2006. Optical properties and electronic structures of $(4CuInSe_2)_y(CuIn_5Se_8)_{1-y}$. Phys. Rev. B 74, 085212.
Hedler, A., et al., 2005. Boundary effects on the plastic flow of amorphous layers during high-energy heavy-ion irradiation. Phys. Rev. B 72, 054108.
Joshi, R.A., et al., 2011. Nanostructured p-$CuIn_3Se_5$/n-CdS heterojunction engineered using simple wet chemical approach at room temperature for photovoltaic application. Mater. Chem. Phys. 127, 191.
Kehan, Y., et al., 2009. Enhancing Solar Cell Efficiencies through 1-D Nanostructures. Nanoscale Res. Lett. 4, 1.
Kessler, J., et al., 2003. Cu(In,Ga)Se_2 thin films grown with a Cu-poor/rich/poor sequence: growth model and structural considerations. Prog. Photovoltaics Res. Appl. 11, 319.
Kilarkaje, S., et al., 2011. Effect of 8 MeV electron irradiation on the optical properties of doped polymer electrolyte films. J. Phys. D: Appl. Phys. 44, 105403.
Krasheninnikov, A.V., et al., 2010. Ion and electron irradiation induced effects in nanostructured materials. J. Appl. Phys. 107, 071301.
Kucheyev, S.O., et al., 2011. Light-ion-irradiation-induced thermal spikes in nanoporous silica. J. Phys. D: Appl. Phys. 44, 085406.

Kuznetsov, M.V., et al., 2003. Evolution of $CuInSe_2$ (112) surface due to annealing: XPS study. Surf. Sci. 530, 297.
Mallick, P., et al., 2012. Evolution of microstructure and crack pattern in NiO thin films under 200 MeV Au ion irradiation. Radiat. Phys. Chem. 81, 647.
Mallick, P., et al., 2008. Swift heavy ion irradiation induced texturing in NiO thin films. Nucl. Instrum. Methods Phys. Res., Sect. B 266, 3332.
Matsumura, S., et al., 2005. Morphological change in FePt nanogranular films induced by irradiation with 100 keV He ions. Scr. Mater. 53, 441.
Ming, X.C., et al., 2006. Nonlinear shift of the Raman A_1 mode in Ga-incorporated $CuInSe_2$ thin films. Chin. Phys. Lett. 23, 1002.
Mobarak, M., et al., 2008. Electrical and thermoelectric properties of $CuInS_2$ single crystal. Mater. Chem. Phys. 109, 287.
Moll, S., et al., 2010. Swift heavy ion irradiation of pyrochlore oxides: electronic energy loss threshold for latent track formation. Nucl. Instrum. Methods Phys. Res., Sect. B 268, 2933.
Parthiban, S., et al., 2011. Effect of Li^{3+} heavy ion irradiation on the Mo doped In_2O_3 thin films prepared by spray pyrolysis technique. J. Phys. D: Appl. Phys. 44, 085404.
Persson, C., et al., 2003. Anomalous grain boundary physics in polycrystalline $CuInSe_2$: the existence of a hole barrier. Phys. Rev. Lett. 91, 266401.
Prakash, J., et al., 2011. Synthesis of Au nanoparticles at the surface and embedded in carbonaceous matrix by 150 keV Ar ion irradiation. J. Phys. D: Appl. Phys. 44, 125302.
Sathyamoorthy, R., et al., 2006. Structural and photoluminescence properties of swift heavy ion irradiated CdS thin films. Sol. Energy Mater. Sol. Cells 90, 2297.
Sato, Y., et al., 2005. Multilayer structure photovoltaic cells. Opt. Rev. 12, 324.
Scheer, R., et al., 2010. Advanced diagnostic and control methods of processes and layers in CIGS solar cells and modules. Prog. Photovoltaics Res. Appl. 18, 467.
Sharma, R., et al., 2009a. Growth of nanocrystalline $CuIn_3Se_5$ (OVC) thin films by ion exchange reactions at room temperature and their characterization as photo-absorbing layers. Appl. Surf. Sci. 255, 8158.
Sharma, R., et al., 2009b. Room temperature synthesis of nanostructured mixed-ordered-vacancy compounds (OVCs) and chalcopyrite $CuInSe_2$ (CIS) thin films in alkaline chemical bath. J. Phys. D: Appl. Phys. 42, 055313.
Shay, J.L., et al., 1973. Electronic structure of $AgInSe_2$ and $CuInSe_2$. Phys. Rev. B 7, 4485.
Shirai, M., et al., 2009. Morphological change in FePt nanogranular thin films induced by swift heavy ion irradiation. Nucl. Instrum. Methods Phys. Res., Sect. B 267, 1787.
Srikar, V.T., et al., 2003. Micro-Raman measurement of bending stresses in micromachined silicon flexures. J. Microelectromech. Syst. 12, 779.
Srivastava, P.C., et al., 2003. AFM studies of swift heavy ion-irradiated surface modification in Si and GaAs. Radiat. Meas. 36, 671.
Tanaka, T., et al., 2003. Effect of 8 MeV electron irradiation on electrical properties of $CuInSe_2$ thin films. Sol. Energy Mater. Sol. Cells 75, 115.
Tanino, H., et al., 1992. Raman spectra of $CuInSe_2$. Phys. Rev. B 45, 13323.
Trautmann, C., 1999. Modifications induced by swift heavy ions. Bull. Mater. Sci. 22, 679.
Wolf, I.D., 1996. Micro-Raman spectroscopy to study local mechanical stress in silicon integrated circuits. Semicond. Sci. Technol. 11, 139.
Yan, Y., et al., 2006. Grain boundary physics in polycrystalline $CuInSe_2$ revisited: Experiment and Theory. Phys. Rev. Lett., 96; p. 205501.
Yoon, S., et al., 2009. Nanoparticle-based approach for the formation of CIS solar cells. Sol. Energy Mater. Sol. Cells 93, 783.
Zaretskaya, E.P., et al., 2007. Correlation between Raman spectra and structural properties of $Zn_{2-2x}Cu_xIn_xSe_2$. Opt. Spectrosc. 102, 77.
Zaretskaya, E.P., et al., 2003. Raman spectroscopy of $CuInSe_2$ thin films prepared by selenization. J. Phys. Chem. Sol. 64, 1989.